Non-destructive measurements for the evaluation of the air permeability of concrete structures

Stéphane Multon, Jérôme Verdier, Géraldine Villain, Hognon Sogbossi, Xavier Dérobert, Hugo Cagnon, Jean-Paul Balayssac

Title Page with Author Information

Authors:

Stéphane Multon [a]*, Jérôme Verdier [a], Géraldine Villain [b], Hognon Sogbossi [a], Xavier Derobert [b], Hugo Cagnon [a] and Jean-Paul Balayssac [a]

(a) *Université de Toulouse; UPS, INSA; LMDC (Laboratoire Matériaux et Durabilité des Constructions); 135, avenue de Rangueil; F-31 077 Toulouse Cedex 04, France*

(b) *Université Gustave Eiffel, MAST – LAMES, Campus de Nantes, allée des ponts et chaussées - CS 5004, F-44-344 Bouguenais Cedex, France*

Non-destructive measurements for the evaluation of the air permeability of concrete structures

Abstract

In the domain of inspection of civil structures, the evaluation of permeability in the field is a major problem of durability for all engineering structures using concrete. Specifically, tightness of the enclosure vessels of nuclear plants has to be controlled regularly. The work presented here aims to estimate the capability of non-destructive techniques (permeameters, capacitive and resistive techniques) to evaluate the leakage flow of concrete structures during their service life or after mechanical, hydric and thermal damage induced by accidental loading. The methodology followed to reach this objective is based on three scales, from laboratory samples to real structures, with an intermediate step on large concrete slabs. The analysis highlights the interest of combining permeability, capacitive and resistive measurements for the evaluation of the air tightness of concrete in the field. Global measurements, performed on large slabs in steady state, and evaluation on representative specimens by Cembureau and the surface permeameter, were in accordance for most of the situations analysed in this work. From the saturation degree evaluated by permittivity and resistivity, it was possible to evaluate the apparent permeability of concrete by means of a van Genuchten law calibrated in the laboratory on representative specimens of the structural concrete.

Keywords

Concrete, Permeability measurement, Permittivity, Resistivity

1 Introduction

The durability of concrete structures can be improved by the use of materials with low transfer properties. Quantifying the permeability and diffusion properties of concrete in the field is thus a major issue for civil engineering research. In addition, the air-tightness of the enclosure vessels of nuclear plants has to be tested regularly during the service life of the structures, approximately every 10 years [1,2]. Measuring permeability in the field is a complex task due to the large size of structures (more than 9000 m² of surface for walls with a thickness of approximately 1 metre) and to the number of zones where leaks can potentially occur. Local measurements of concrete permeability can be of great help in completing global measurements on the entire vessel: they improve our knowledge of the heterogeneity of the leaks in the structures and thus help to predict the zones where impermeability may be poor, and to monitor it regularly with a minimum of disturbance to usual operation.

Air permeability can be measured in laboratory [3] on specimens drilled from the structures, but such test leads to partial degradation of the structure and non-destructive techniques are usually preferred. Thus, different techniques were developed to measure the air permeability in situ [4–8]. Torrent proposed a device which can be fixed on the surface of the concrete without any holes by vacuum technique [4,9]. The permeability is measured during the unsteady state of the increase of pressure in a cell [4,9]. This paper proposes the comparison of different techniques of air permeability measurement in laboratory for a use in field.

Air permeability is highly dependent on the moisture present in the concrete [10,11] and various non-destructive techniques can be used to determine the saturation degree in porous material, such as resistivity and permittivity [12–18]. The use of such techniques in field is a great challenge. If the dependence of air permeability on saturation degree is known, it is then possible to evaluate the concrete permeability in the field from resistivity or permittivity measurements. It is the second main goal of this paper.

Thus, the purpose of this paper is to test the capability of various non-destructive techniques (permeameter devices, capacitive and resistive techniques) to evaluate the leakage flow of concrete structures during their service life or after accidental loading. The methodology used to reach this objective is based on tests at three scales:

- On usual laboratory samples: preliminary test of the surface permeability technique (samples with diameter 150 mm and thickness 50 mm) and comparison with the reference concrete permeability test (Cembureau permeameter) for different saturation levels; calibration tests of the capacitive and resistive techniques on samples drilled from concrete slabs (samples with diameter 75 mm and thickness 70 mm);
- On large laboratory slabs: validation of the calibration obtained on samples in laboratory conditions (slabs with dimensions 125 x 250 x 500 mm),
- In field: comparison of the three techniques on a part of the Vercors mock-up built by EDF to help in the management of the long-term operation of its fleet of Nuclear Power Plants [19,20].

The conclusions of this work are not only useful for checking the tightness of structures for nuclear uses. They also confirm the interest of the different techniques used here for following up the durability properties of concrete in the field.

2 Techniques and materials

2.1 Experimental programme

The objective of the experimental programme was to evaluate the capacity of three non-destructive techniques (based on direct permeability measurement with a surface permeameter and on measurements of the saturation degree by resistivity or permittivity measurements) to quantify the concrete permeability in the field. The programme was divided into three steps.

First, usual laboratory samples (diameter 150 mm and thickness 50 mm or diameter 75 mm and thickness 70 mm) were compared and calibrated on laboratory specimens for different saturation degrees: from totally saturated concrete to concrete dried under severe conditions (105°C until the mass of the specimen became constant). Under these conditions, significant cracking could occur and impact the measurements [21,22].

Secondly, the techniques were validated on large laboratory slabs (125 x 250 x 500 mm) under different environmental conditions, to represent concrete during the service life of structures (in concrete with high degrees of saturation in stress-free or loaded conditions) or after accidental expositions (damaged by thermo-hydric loading). Four types loading can be distinguished (based on the assumption that the average saturation degree of the concrete of usual enclosure vessels is about 60% [20]):

- Hydric loading: slabs were subjected to drying at 60 °C to obtain 60 and 30% of saturation,
- Mechanical loading: slabs at 60% saturation were subjected to uniaxial compressive loading of between 0 and 12 MPa (because enclosure vessels are subjected to about 12 MPa of compressive prestressing in the orthoradial direction and to about 7 MPa in the vertical direction),
- Thermal loading: sealed slabs at 60% of saturation were subjected to 80 °C for 14 hours in endogenous conditions (without loss of mass),
- Thermal-hydric loading: slabs at 60% of saturation were subjected to 150 °C or 200 °C for 14 hours.

The first two types of loading occur during the service life of the structure, while the last two can occur during accidental situations.

96 In the third step, the three techniques were used on a part of the Vercors mock-up. The
97 saturation degree and the values of concrete permeability evaluated by each technique were
98 compared and discussed.

99 **2.2 Experimental techniques**

100 *2.2.1 Permeability measurements*

101 Three techniques for permeability measurement were used in this work. The evaluation of
102 tightness of the enclosure vessel of a nuclear power plant during usual enclosure tests is based
103 on the measurement of air leakage under 5.2 bars of internal pressure in the whole structure,
104 corresponding to the evaluated pressure reachable in case of accident. In order to complete
105 this global test, local permeability measurement of concrete [4–8] seems to be the most
106 natural option.

107 Usually, concrete permeability is measured in the laboratory by the Cembureau method [3]
108 (Figure 1). The principle is to determine the permeability under pressure during steady flow.
109 The result can be directly used to evaluate the leakage of structures in field. The Cembureau
110 technique is the only method standardized for the measurement of concrete permeability on
111 laboratory specimens but it cannot be used in the field because the tested samples have to be
112 confined to control the air flow. In this work, laboratory specimens were first used to
113 characterize the concrete and compare the different techniques. Cembureau apparent
114 permeability measured for 2 bars of absolute pressure was the first permeability technique
115 used in this work. As this method is standardized, it was chosen to be the reference
116 permeability.

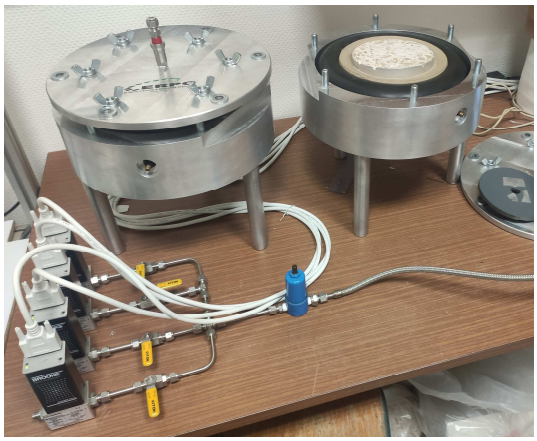

Figure 1: Cembureau apparatus for concrete permeability measurement in laboratory

For this study, a second method able to evaluate permeability in the field was necessary. The permeameter proposed by Torrent [4] was used (Figure 2). As this test is based on a vacuum technique and unsteady flow, specific relations [23–26] are necessary so that the permeability deduced from this measurement can be compared to that found with the Cembureau method. The principle of the method to obtain comparable permeability with Torrent and Cembureau permeameters is presented in the following section. As the Torrent permeameter is based on air flow in an unsteady state, the numerical determination of the permeability is not exact, unlike the method using steady flow [23].

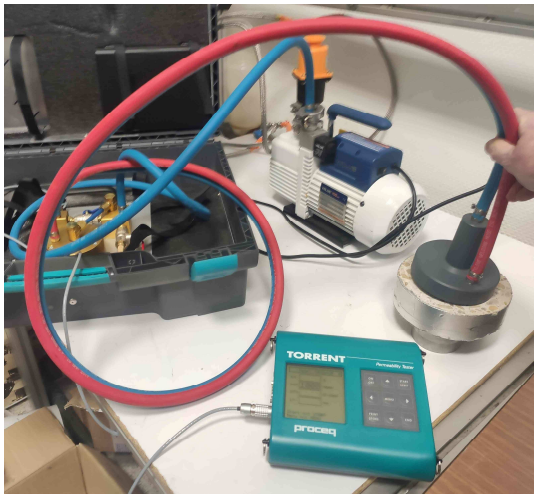

Figure 2: Torrent apparatus for concrete permeability measurement in field

125 Permeability measurement was also performed on the large laboratory slabs under steady
126 flow. The merit of this technique is to evaluate air permeability on volume representative of
127 small structures. Due to potential leakage, measurements of permeability under pressure were
128 difficult to perform on the large slabs used in the second step of the methodology presented.
129 On such large slabs, air-tightness was easier to obtain for measurement in a vacuum.
130 However, it was necessary to use PVC plates stuck and made tight with silicone glue directly
131 on the lateral faces of the slab to obtain a correct sealing. The conditioning was long and
132 needed frequent verification of the sealing. Thus, the air permeability of all the slabs could not
133 be measured in the program. After sealing of the lateral faces of the slabs, a vacuum was
134 applied in a cell glued to one face of the slab (250 x 500 mm). On the opposite face (250 x
135 500 mm), the air flow was measured in the steady state to obtain the air permeability of the
136 whole concrete slab measured in vacuum. The relation necessary to evaluate the permeability
137 under pressure from the measurement in vacuum is presented in [24]. The permeability thus
138 measured was used to validate all the non-destructive methods on the concrete slabs. This
139 third technique is named 'double-cell' in the rest of the paper.

140 *2.2.2 Non-destructive techniques for determination of the saturation degree*

141 In this work, resistivity and permittivity techniques were used to determine first the saturation
142 degree of the concrete and then to deduce the air permeability from the measured saturation
143 degree.

144 Resistivity is measured by a Wenner probe (Figure 3) consisting of four electrodes placed a
145 distance 'a' apart (a =40 mm). The two outer electrodes inject a direct current, I, while the
146 two inner ones measure the difference of potential, ΔV. The resistivity, ρ, is calculated by the
147 relation [27]:

$$\rho = 2.\pi.a.\frac{\Delta V}{I} \qquad \textit{Eq. 1}$$

148 The resistivity probe used in this work investigated a depth of concrete of about 15 mm.

Figure 3: Apparatus for concrete resistivity measurement

149 Permittivity measurement uses a device composed of two (or more) electrodes on the outer
150 surface of the concrete (Figure 4). An alternating electric current is applied between the
151 electrodes and so the concrete acts as a capacitor. Any change of concrete capacitance induces
152 a shift in the resonant frequency (around 33 MHz) of the system. This change of capacitance
153 is linked to the change of permittivity of the concrete induced by moisture variation [15]. The
154 apparatus used in this work investigated a depth of concrete of about 15 mm [28].

155

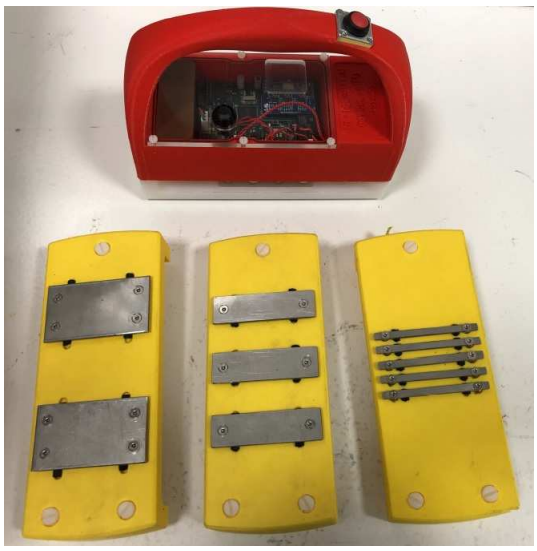

156

Figure 4: Apparatus for concrete permittivity measurement

157 These last two techniques were applied on the surface of the slabs (500x250x120 mm) as well
158 as on the reinforced structure of the Vercors mock-up. Meanwhile, the calibration tests on
159 small samples (75x70 mm) were performed by means of cylindrical cells following the
160 protocol described in [29].

161 **2.3 Concrete and conditioning**

162 Concrete used in this work (Table 1) is representative of a wide range of concrete used in
163 French nuclear plants. The mix-design was similar to the concrete used for the Vercors mock-
164 up built by EDF with usual siliceous limestone aggregates (silica contents of 80% and 5% for
165 the sand and the gravels, respectively). Samples and slabs were cured in lime water at a
166 temperature of 20 ± 2 °C for at least 60 days after casting to obtain a stabilized material
167 regarding cement hydration [30]. The mean compressive strength and instantaneous modulus
168 of the concrete were respectively 49 MPa and 35.3 GPa, with coefficients of variation of
169 about 10%.

170

171 **Table 1.** Concrete mix

Constituents	**[kg/m^3]**
Sand 0/4	830
Gravel 4/11 R	445
Gravel 8/16 R	550
Cement CEM I 52.5 NCE CP2 NF	320
Plasticizer	2.4
Water	167

172

173 Experiments were performed on usual laboratory samples (diameter 150 mm and thickness
174 50 mm), on large laboratory slabs (125 x 250 x 500 mm) and on cores (diameter 75 mm and
175 thickness 70 mm) drilled from slabs. Fourteen slabs, made from three concrete batches, were
176 used. In the following, they are referenced as Bi-j, where 'i' is the reference of the batch and
177 'j', the reference of the slab in the batch.

178 In this study, the saturation degree of all the samples and slabs was controlled. The
179 conditioning, inspired from [29,31–34], was intended to limit thermo-hydric gradients and
180 resulting skin cracking. The small samples were first saturated under vacuum. Then, they
181 were dried with a gradually increasing drying temperature (40 °C to obtain 80% saturation, 50
182 °C to obtain 60%, 45%, 30% and 10%, and 105 °C to reach the smallest degree of saturation,
183 taken as 0% in this work). Targeted masses were evaluated from the porosity measured on
184 other samples cast from the same concrete batch and, once the target mass was reached, the
185 test samples were placed in sealed conditions (aluminium and sealed bags). They were put
186 back into the oven (for a period at least equal to the drying time) in order to partially
187 homogenize the water distribution throughout the sample and thus minimize the impact of
188 moisture gradient on measurements [34].

189 To evaluate the impact of elevated temperatures on the concrete properties, some samples and
190 slabs were subjected to thermal loading in an oven preheated to 80, 150 and 200 °C for 14
191 hours. Before the thermal loading, samples and slabs were wrapped in watertight aluminium.

Fourteen hours were necessary to reach the target temperature in the slab cores and to maintain this temperature for two hours, as evaluated during the ENDE project [35]. All the properties were measured after the return to ambient temperature. Cylindrical samples (75x70 mm) were cored in the slabs (with or without thermal damage) to evaluate the effect of the thermal loading level on NDT results. Control of the saturation degree was applied to all specimens as previously described (the target was usually obtained with an accuracy of about 2% of saturation degree).

2.4 Air permeability of reference concrete according to saturation degree

The question that arises in this work concerns the capacity of different techniques to allow the air permeability through concrete to be measured in the field. This work can also be used to evaluate the ability of usual laboratory techniques applied to small samples to give an evaluation representative of concrete permeability in real structures.

As the Cembureau technique [3] is standardized and commonly used in the laboratory, the apparent permeability of concrete to air, measured by this technique using 2 bars of absolute pressure, is used as a reference for all the work presented here.

The evolution of the reference permeability with the saturation degree of concrete is given in Figure 5 for three specimens. The measurements present scatter that is usual for air permeability measurements. The usual variation of air permeability of concrete with the saturation degree [10] can be observed.

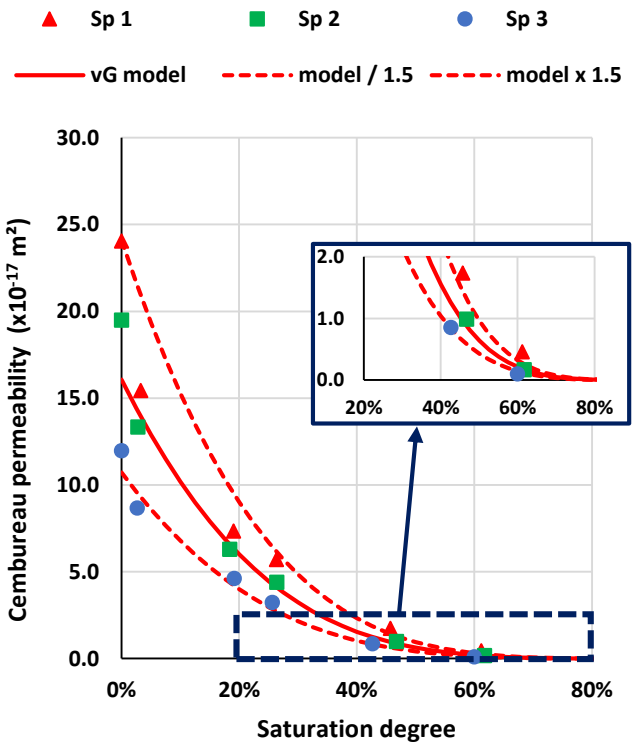

211

212 *Figure 5: Concrete permeability measured by Cembureau technique according to the degree of saturation of*
213 *concrete and van Genuchten's law calibrated on the measurements (red dashed lines represent a variation of*
214 *50% of the value obtained by the calibrated model)*

215 The dependence of the air permeability of concrete on saturation degree can be evaluated by
216 van Genuchten's law [36,37], initially defined for soil and later transposed to concrete:

$$k_{S_r} = k_0.(1 - S_r)^q(1 - {S_r}^{1/m})^{2m} \qquad \textit{Eq. 2}$$

217 where k_{S_r} is the apparent permeability for a given saturation degree S_r and k_0 the apparent
218 permeability for the driest saturation degree (obtained in this programme after drying at 105
219 °C). q and m are the van Genuchten parameters, which depend on concrete transfer properties.
220 Van Genuchten parameters, q and m, are determined by calibration of the equation on the
221 experimental values of permeability obtained for different saturation degrees.
222 The interest of this technique is to measure air permeability in perfect controlled conditions
223 (unidirectional air flow and steady state). The permeability is thus calculated from the

theoretical solution of the transfer problem. However, it can only be performed on specimens in laboratory. For structural concrete, it can only be performed on specimens drilled from the structure leading to partial degradation.

Two of the techniques used in this work are able to evaluate the saturation degree of concrete (resistivity and permittivity). Combined with the van Genuchten law evaluated from laboratory measurements, they can be used to evaluate the air permeability of concrete in the field.

For usual environmental expositions, the concrete saturation often lies between 30 and 50% at the surface and is often higher in the core of massive structures [20]. Thus, it was chosen to calibrate van Genuchten' law with very low weight (5%) for the two driest saturation degrees (0 and 3%), which are not representative of the humidity state during the service life of usual structures. This gives an evaluation in accordance with measurements of high saturation degrees (see the detail in Figure 5) with correct evaluation of air permeability for the two lowest saturation degrees (Figure 5). The calibration leads to 16.1×10^{-17} m^2, 4.2 and 0.5 for k_0, q and m respectively (the mean deviation between the experimental results and the calibrated equation is about 30% – the correlation coefficient is about 0.94). All the experimental values are located between two lines, which represent the model multiplied or divided by a factor of 1.5. Such discrepancy is usual for concrete air permeability measurements [37].

3 Experimental results

3.1 Comparison and calibration of NDT for permeability evaluation

The first step of the methodology used here is based on preliminary tests of the three techniques on usual laboratory samples. The aim is to compare or to calibrate the three non-destructive techniques with the reference concrete permeability test presented just above.

3.1.1 Comparison of permeability techniques: laboratory and in the field measurements

The first non-destructive technique used in this work is a technique of measurement of permeability performed at the surface of concrete [4]. For such permeameters, the air flow is obtained with the vacuum technique. First, a vacuum is imposed for 60 seconds in a cell in contact with the concrete surface. Then, the vacuum pump is stopped and the permeability is evaluated during the unsteady state of the increase of pressure in the cell [4]. The merit of this technique lies in its capacity to evaluate concrete permeability in field without any degradation of concrete (the device is attached to the structural concrete thanks to vacuum). However, as the permeability is evaluated during an unsteady state, no exact mathematical solution exists for this physical problem [4]. Simplifying assumptions are thus necessary to assess this transfer property. They lead to numerical approximations for the permeability obtained with such a technique.

Yssorches et al. proposed a measurement of permeability based on a vacuum technique in the laboratory [38]. The technique was based on the same principle as the Torrent apparatus (imposing a vacuum on a face of concrete for a certain time, then evaluating the permeability from the pressure increase when the pumping is stopped) but only for fairly thin samples. In such conditions, the permeability evaluated in the first period of pressure increase was not representative of the real permeability. For small samples in the laboratory, the increase became almost linear after a long period of time (at least 15 minutes) and the authors recommend evaluating the permeability from the slope of the increase when the regime is stabilized. For small samples, the stabilization is obtained when the thickness is totally crossed by the air flow. At this time, the profile of pressure is stabilized in the thickness and the regime is pseudo-steady, as indicated in [38]. The regime at the beginning of the pressure increase seems to be disturbed by the modification of the boundary conditions, particularly for a small duration of vacuum [38]. This may be due to the brutal stop of the pumping and

strengthened by a moisture gradient in the concrete skin.

In the case of laboratory samples, once the air flow is almost constant across the concrete thickness, a pseudo-steady regime is set up and the apparent permeability can be deduced from the Hagen-Poiseuille equation and from the conservation of the air mass between the concrete porosity and the volume of the cell [23,39]:

$$k_{a\_psr} = \frac{2 \cdot \mu \cdot L}{A \cdot (P_{atm}^2 - P_c^2)} \cdot V_c \cdot \dot{P}_c \qquad \textit{Eq. 3}$$

with k_{a_psr} the apparent permeability (m²) obtained during the pseudo-steady regime (there is no real steady regime in this test as the pressure in the cell increases with time, but the gradient of pressure between the two surfaces of the sample is almost constant as the increase of pressure in the measurement cell is small during the test), μ, the air viscosity (Pa.s), L, the thickness of the samples (m), A, the sample cross-section (m²), P_{atm}, the atmospheric pressure (Pa), V_c, the volume of the cell (m^3), P_c, the pressure in the cell (Pa) and $\dot{P}_c$, the slope of the pressure increase in the cell ($Pa.s^{-1}$). Following the recommendations of Yssorche et al.[38], the slope $\dot{P}_c$ was evaluated in the present work for the last minutes of the pressure increase (over a duration of 120 seconds).

For large concrete thickness, the duration of vacuum time would be too long to expect to perform a permeability measurement in such controlled conditions. The main difficulty is then to evaluate the depth of concrete impacted by the air flow. In his approach, Torrent proposed to evaluate this depth, L_0, from the mass balance of air moles crossing concrete to reach the central cell during the test [4]:

$$L_0 = \sqrt{\frac{2 \cdot k_{a\_t} \cdot P_{atm} \cdot (t_v + t)}{\varphi \cdot \mu}} \qquad \textit{Eq. 4}$$

with: k_{a_t} (m²) the unknown permeability of the concrete crossed by the air flow; t_v the

vacuum time; t the time after the cessation of pumping; φ the porosity of concrete; and μ (Pa.s) the air viscosity.

By combining the two previous equations, it is possible to evaluate the permeability, k_{a_t}, from the slope of the pressure increase in the central cell for any time, t, after the pumping stops, by the following equation:

$$k_{a\_t} = \frac{8 \cdot \mu}{\varphi} \cdot \left(\frac{V_c}{A}\right)^2 \cdot \frac{P_{atm}}{(P_{atm}^2 - P_c^2)^2} \cdot \dot{P_c}^2 \cdot (t_v + t) \qquad \textit{Eq. 5}$$

For specimens with small thickness and large permeability, the air flow rapidly becomes almost constant across the concrete (pseudo-steady state). The permeability can be evaluated from Eq. 3. The previous results obtained in the laboratory have shown that the best evaluation of the permeability will be reached for a long testing time in this case [38]. For specimens with intermediate permeability, the air flow can cross the thickness (so only the external surface is at atmospheric pressure), but the duration of the pressure increase is too short to reach the pseudo-steady state. In this case, evaluating the permeability by Eq. 3 will lead to an overestimation [38]. For specimens with large thickness or small permeability, the air flow does not cross the specimen thickness (a part of the concrete inside the sample is still at atmospheric pressure). The permeability is then evaluated by Eq. 5. If Eq. 5 is used, the evaluation of the permeability is based on the evaluation of the depth of the concrete investigated, L_0 (Eq. 4). The evaluation is based on simplified assumptions and particularly on the linearity of pressure at a certain depth of concrete [4]. The profile is not really linear throughout this depth and this will lead to a misestimation of the permeability.

Permeability was measured by the Torrent apparatus for the different degrees of saturation on the sample surface, for the same samples as those used in the Cembureau tests (Figure 5) and the surface permeability was evaluated by the method presented just above. Most of the samples with saturation degrees equal to or lower than 30% were crossed by the air flow

during the measurements (permeability evaluated by Eq. 3). None of the samples with higher saturation degrees were crossed by the air flow (permeability evaluated by Eq. 4 and Eq. 5).

Vacuum techniques are commonly used for measuring concrete permeability [4,26,38]. The mean free path of particles during air flow in a vacuum is different from the mean path under pressure [40]. The difference has to be considered to evaluate permeability under pressure from permeability measured in a vacuum, as proposed in [23,24]. For the concrete used in this work, the apparent permeability for 2 bars of absolute pressure could be deduced from measurement in vacuum by using a proportionality factor, C_P, of about 0.57 [23]. Figure 6 compares the permeability evaluated by the Cembureau test (under pressure in steady state) and the permeability evaluated by surface measurement (in vacuum in unsteady state) corrected for the difference of pressure (coefficient C_P).

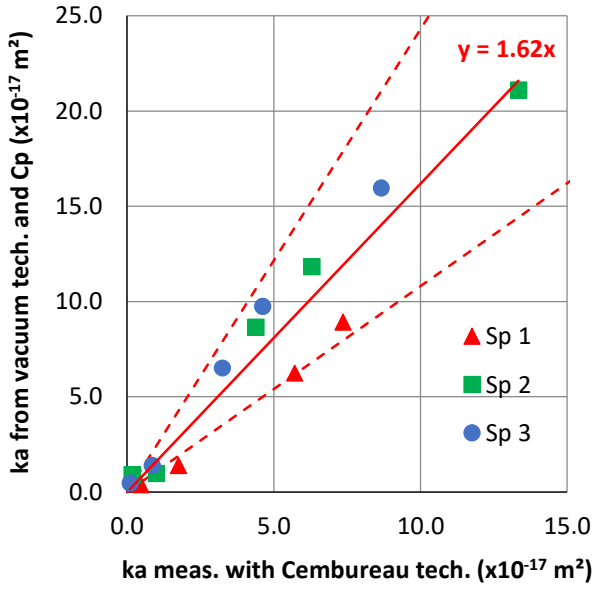

Figure 6: Comparison between the permeability obtained by Cembureau technique for 2 bars of absolute pressure and the surface permeability obtained by Torrent apparatus, evaluated by Eq. 3 and Eq. 5 and corrected with pressure (red dashed lines represent a variation of 50% of the value obtained by the linear equation)

The method leads to an overestimation of the apparent permeability of about 60%. Such a result could be expected due to the short duration of the vacuum (60 seconds) and the short duration of the measurement of the pressure increase (to a maximal increase of 20 mbars) in the central cell of the apparatus (up to 720 seconds of pressure increase). This overestimation is in accordance with the results obtained previously on samples in the literature [38]. The dispersion (ratio of 1.5) is acceptable in comparison with the usual scatter observed for permeability obtained by the Cembureau technique (Figure 5). Works are in progress to validate this approach for other concrete mix-designs.

3.1.2 Calibration of permittivity for permeability evaluation

Permittivity can be used to evaluate the saturation degree of concrete [15,16]. By combining it with van Genuchten's law evaluated from laboratory measurements (Figure 5), it is then possible to deduce the concrete permeability.

The linear dependence of permittivity on saturation degree was evaluated from samples drilled from six slabs before thermo-hydric loading (Figure 7-a). Before loading, slight differences can be observed between the measurements performed on samples taken from the core of the slabs and those taken from the surface (Figure 7-a). They are due to surface effects during casting or ageing, because the surface measurements integrate the properties of the concrete skin, which are different from the properties of the concrete core. The calibration curve obtained on samples representing the surface was preferred for the measurements on slabs and on the Vercors mock-up. Figure 7-b shows the concrete permittivity before (60 °C) and after thermo-hydric loading (150 °C and 200 °C) obtained on cores that were reconditioned after the loading to obtain the measurements on concrete with four different saturation degrees. The damage induced by this loading did not lead to significant differences in concrete permittivity, while the consequences on air permeability were considerable, particularly at high saturation [22].

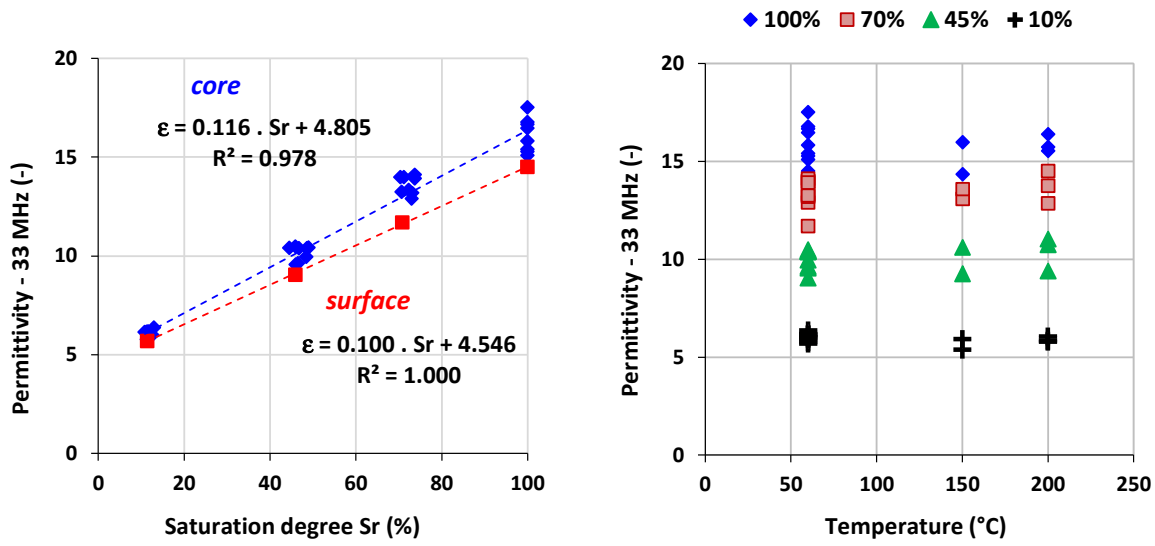

(a) (b)

357 *Figure 7: Calibration of permittivity with the saturation degree (a) and impact of thermo-hydric loading on*
358 *concrete permittivity (b)*

359 From the equations obtained by the calibration of permittivity (Figure 7) and the van
360 Genuchten law obtained from the Cembureau technique (Eq. 2 - Figure 5), it is possible to
361 evaluate the concrete permeability and permittivity from the saturation degree (red and blue
362 lines in Figure 8 for surface and core calibration respectively). Such evaluations can be
363 compared to permeability measurements obtained by the Cembureau method (data in Figure
364 8).

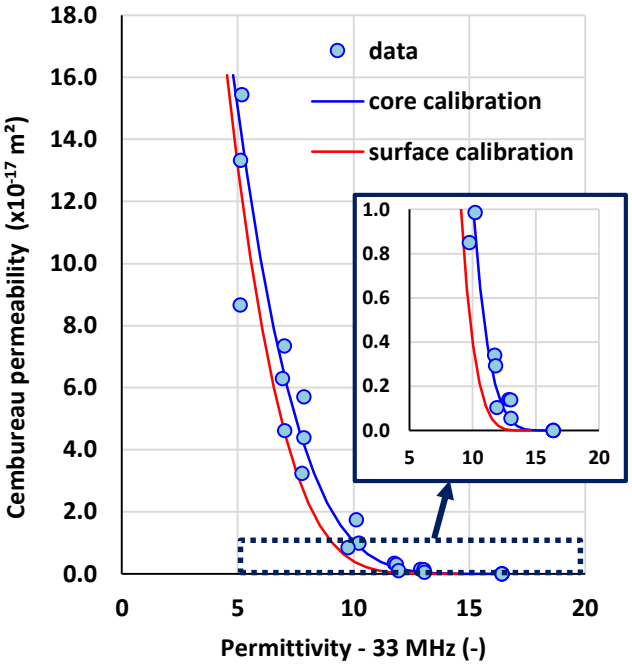

365

366 *Figure 8: Evaluation of permeability from permittivity through van Genuchten's law with the calibrations*
367 *obtained on samples drilled from the surface and from the core of laboratory slabs*

368 As the calibration was not performed on the same specimens as used for Cembureau tests, this
369 comparison shows the good reproducibility between the different batches of concrete used for
370 specimens and for slabs in terms of transfer properties. It also validates the method for the
371 evaluation of permeability from permittivity on laboratory samples. However, the evaluated
372 permeability is greatly modified for small variations of permittivity in the range of 5-7 (Figure
373 8), which corresponds to degrees of saturation lower than 20%. The important interest of this
374 technique is to be able to evaluate the saturation degree of concrete for a large range of
375 saturation degree (from 0.2 to 1.0) without any degradation of the structure. However, under
376 20% of saturation, a small difference of permittivity can lead to a large difference in deduced
377 permeability. This is not relevant for most of the service life of civil engineering structures
378 but it can be reached after accidental exposure.

3.1.3 Calibration of resistivity for permeability evaluation

The same method was used for resistivity measurement as for permittivity. First, the calibration was performed on laboratory samples so as to be able to evaluate the saturation degree of concrete from resistivity (Figure 9-a). For resistivity, the calibration was performed for high saturation degrees (higher than 45%) as water has to be sufficiently connected in the porosity if concrete resistivity is to be measured. Measurements were performed on samples taken from the core of the slabs and on samples taken from the surface. Few differences were noted between the samples and it was decided to calibrate only one equation for all the measurements (Figure 9-a). As for permittivity, small differences were also observed for the concrete resistivity before and after the thermal loading (Figure 9-b). For high saturation degrees (100%), resistivity was similar for all the samples. For 70% and 45% of saturation, noteworthy scatter was observed for the samples before temperature exposure. The samples came from two different batches, which can partly explain the scatter. Moreover, for 45% of saturation, small differences of the saturation degrees (which were between 44.5 and 49% according to the samples) have a large impact on the resistivity value. The resistivity technique presents the same limit as permittivity but for higher saturation degrees (from about 0.5 to 1.0). Moreover, as the conversion model from resistivity to saturation degree is a power function, small variation of low values of resistivity can lead to higher uncertainties for high degrees of saturation ($0.9 < Sr < 1$) than for low degrees of saturation ($0.5 < Sr < 0.6$). This is not the case for permittivity measurements because the conversion model is linear. However, a slight decrease in concrete resistivity can be noted with the temperature of thermo-hydric loading. The decrease in resistivity can be explained by the effect of the cracking induced by the loading. Cracks can lead to new paths of transfer in the concrete and thus to a resistivity decrease. In this experimentation, it is mainly significant for the saturation degree of 45%.

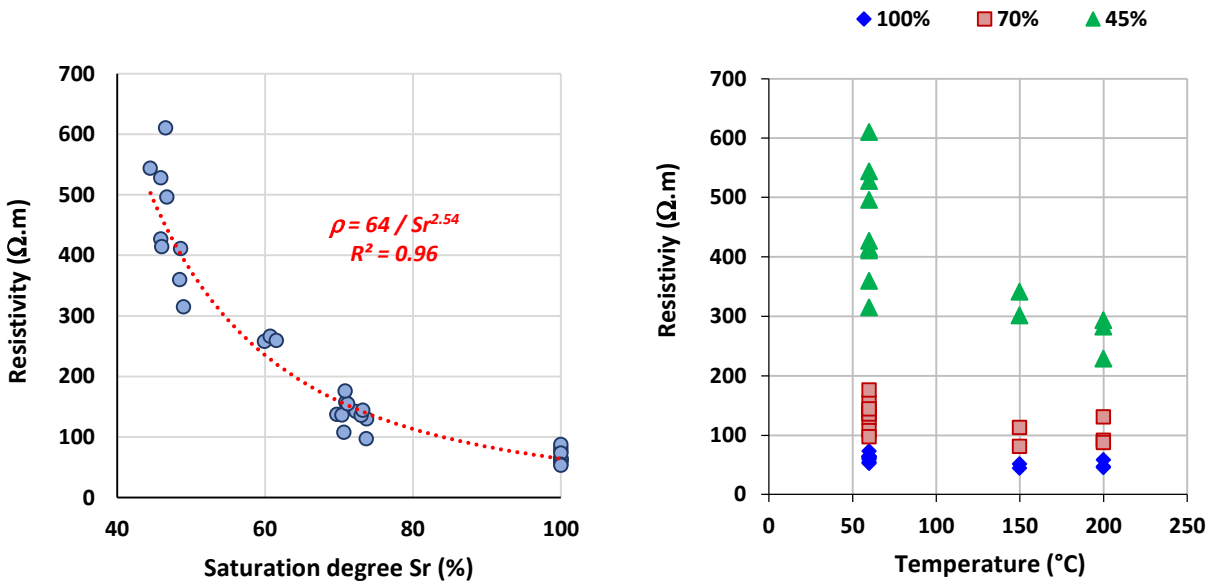

(a) (b)

403 *Figure 9: Calibration of resistivity with the saturation degree (a), and impact of thermo-hydric loading on*
404 *concrete resistivity (b)*

405 From the calibration of resistivity (Figure 9) and the van Genuchten law obtained from the
406 Cembureau technique, it is possible to extrapolate the evolution of concrete permeability with
407 resistivity for a higher domain of saturation degrees (Figure 10), in accordance with
408 measurements performed in the field in the last part of this paper.

409

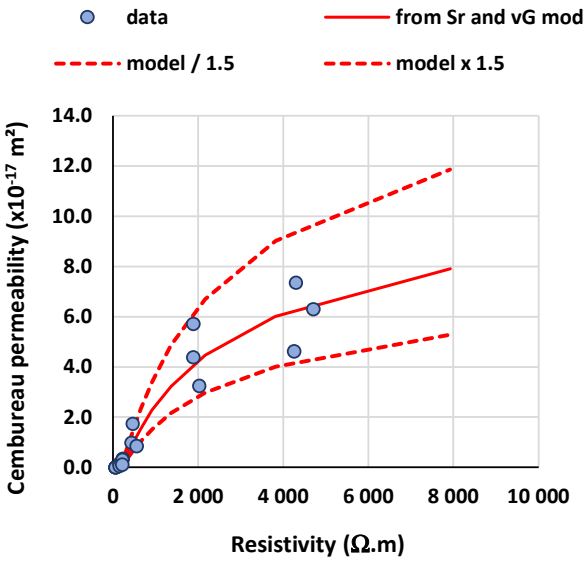

410

411 *Figure 10: Evaluation of permeability from resistivity through van Genuchten's equation and linear empirical*
412 *model (red dashed lines represent a variation of 50% of the value obtained by the calibrated equation)*

413 **3.2 Validation on large laboratory slabs**

414 The second intermediate step of the methodology was to use the three previous techniques on
415 large laboratory slabs (125 x 250 x 500 mm) with different loadings: hydric, mechanical,
416 thermal and thermal-hydric. The aim was to compare the responses of the three techniques for
417 these different types of loading and, in some cases, to compare them with a direct global
418 measurement of permeability performed in vacuum and steady state on the whole slab across
419 the thickness (flow surface: 250 x 500 mm). The permeability measured on small laboratory
420 samples with the Cembureau permeameter is also represented on all the figures of Section 4 to
421 enable a direct comparison of permeability determined on slabs and permeability obtained
422 during the first characterization on samples. Thus, it is possible to draw conclusions on how
423 representative permeability measurements performed on samples in the laboratory can be in
424 evaluations of the permeability of larger elements.

425 *3.2.1 Impact of hydric loading*

426 The saturation degree of concrete in the field can be high in the cores of massive structures
427 and in locations exposed to rainfall. Usually, a large proportion of the concrete of enclosure

vessels has a saturation degree lying between 50 and 60%, but parts of the vessels can be subject to local drying due to external environmental conditions. In this section, concrete slabs first soaked in lime water for at least 60 days were exposed to 50 °C to reach 60% and 30% of saturation. Once the desired saturation was reached, the slabs were wrapped in watertight aluminium. Mass measurements were performed to verify the efficiency of the packing.

Eight slabs were used for this part. The results of measurement for the three non-destructive techniques and for the double-cell technique are given in Table 2. The lowest saturation degree was about 30% and no resistivity was measured on any of the three slabs.

Table 2: Measurements from the different techniques on slabs after hydric loading, and saturation degree (Sr) deduced from permittivity and resistivity

	Slab	**B1-2**	**B3-10**	**B2-9**	**B2-7**	**B1-3**	**B1-4**	**B1-5**	**B1-6**
Sr	*%*	**100**	**60**	**62**	**60**	**59**	**27**	**26**	**25**
Surf. Perm.	$x10^{-17}$ m^2	-	2.55	1.27	4.70	1.9	-	-	-
Permittivity		12.8	10.3	10.5	10.6	8.3	5.9	5.8	6.0
Deduc. Sr	*%*	82.7	57.3	59.3	60.8	43.5	13.8	13.0	14.5
Resistivity	$\Omega.m$	64.6	236.2	201	-	305.3	-	-	-
Deduc. Sr	*%*	99.6	59.8	63.7	-	54.1	-	-	-
Double-cell	$x10^{-17}$ m^2	-	-	-	-	-	10.0	-	-

From the measurements given in Table 2, it is possible to evaluate the apparent permeability at 2 bars as proposed in Section 3. The surface permeability and the double-cell are vacuum techniques. The apparent permeability for 2 bars of absolute pressure can be deduced from the measurements in vacuum by applying a proportionality factor, C_P, of about 0.57 [23]. For the surface permeability, an overestimation of 60% was observed (Figure 6). This overestimation

444 was considered in the evaluation of apparent permeability for 2 bars of absolute pressure by
445 dividing the results by 1.62. For the permittivity and the resistivity, the saturation degree was
446 first evaluated from calibrations performed on laboratory samples (Table 2) and the apparent
447 permeability was then evaluated from van Genuchten's law calibrated on the Cembureau test.
448 The apparent permeabilities for an absolute pressure of 2 bars evaluated by all the techniques
449 are shown in Figure 11-a. Figure 11-b presents the details of the results for the highest
450 saturation degrees.

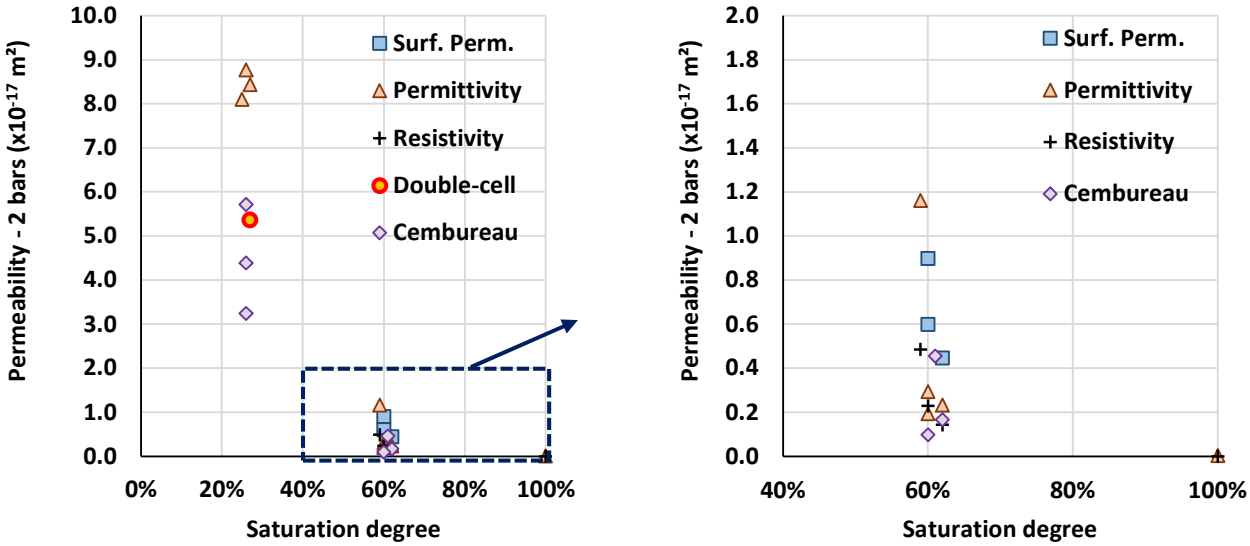

(a) (b)

451 *Figure 11: Evaluation of apparent permeability for an absolute pressure of 2 bars by the different techniques on*
452 *slabs under hydric loading*

453 For 60% of saturation, no direct double-cell measurement was performed, but the evaluation
454 by the different techniques can be compared and confronted to the permeability measured on
455 samples by Cembureau tests (Figure 11-b):

456 - Resistivity and 3 measurements on 4 slabs by permittivity gives an evaluation of the
457 apparent permeability that is of the same order as the permeability measured on
458 samples with the Cembureau technique;

- Surface permeability gives a slight overestimation of the apparent permeability. At 60% of saturation, the aspiration necessary to obtain the vacuum leads to water movements, evaporation and an overestimation of the permeability due to the long time necessary to reach a pseudo steady state. In addition, homogenization of the water distribution in the slab may not be totally completed at the time of measurement [41]. In presence of a moisture gradient, surface permeability can lead to the permeability being overestimated with respect to the Cembureau measurement;
- 3 permittivity measurements on 4 slabs gave a correct estimation of air permeability. Only 1 measurement overestimated the permeability. For this slab, the saturation degree was evaluated at 43.5% by the technique, whereas it was checked at 59%. This shows the sensitivity of this measurement to the test conditions, as is also observed in the following section. This sensitivity seems higher than for the other techniques.

For one slab compared to the other ones, resistivity jumps from about 200 Ω.m to 305 Ω.m for a similar saturation degree (about 60%). This technique is based on the injection of an electrical current in concrete. The electric current is carried by the ions present in the concrete pore solution. It gives reliable results for concrete with high saturation degree (what is usual for massive concrete structures submitted to external environmental conditions) [42]. However, for this concrete, it becomes highly nonlinear under 60%, because the solution is no longer continuous in the concrete porosity. Then the results become highly scattered. This effect should be considered when resistivity measurement is used on structures exposed to dry conditions.

For 30% of saturation, the air permeabilities measured by the double-cell and by the Cembureau technique on samples were consistent. Permittivity measurements showed small dispersion, but the evaluation overestimated the apparent permeability by almost 60% (Figure 11-a). This was due to an underestimation of the saturation degree. Permittivity calibration led

484 to a saturation degree lying between 13 and 14.5 for the three slabs, while it was actually
485 about 25-27% (Table 2). Several difficulties can explain this result:

486 - Permittivity is less sensitive to the saturation degree under 20% because the
487 quantity of water inside the porosity is not great enough [43]. Such conditions of
488 moisture are rare for structures exposed to external conditions, but it is important to
489 highlight the risk of using permittivity in structures exposed to dry conditions without
490 specific consideration [43].
491 - Secondly, to obtain controlled saturation degrees, the slabs were first exposed
492 to drying which leads to moisture gradient. Slabs were then placed in sealed
493 conditions and put back in temperature (for a period of time at least equal to the drying
494 time) in order to homogenize the water distribution throughout the sample. However,
495 movements of water are slower during homogenization than in drying [44]. Thus, the
496 gradient was not totally removed at the end of the period. This effect was greater for
497 the slabs than for small samples. The calibration of the conversion model was
498 performed on small cores with homogenous conditions while measurements on slabs
499 were realized on shuttered surface. It was more difficult to obtain homogenous
500 conditions in reasonable time for the slabs.

501 As the techniques did not investigate the same depth, this conditioning can lead to different
502 scattering between techniques but also, with the global saturation degree obtained by mass
503 measurement.

504 *3.2.2 Impact of mechanical loading*
505 During their service lives, enclosure vessels are subjected to constant compressive stress due
506 to prestressing – usually between 7 and 12 MPa (axial and radial prestressing respectively).
507 For increasing compressive stress lower than 50% of the compressive strength, air
508 permeability of concrete usually shows a slight decrease due to consolidation and pore closing

509 [45,46]. In this work, concrete slabs with 60% of saturation were subjected to compressive
510 stress of between 0.5 and 12 MPa. Due to the small thickness (125 mm) of the slabs compared
511 to their height (500 mm), it was difficult to obtain homogeneous compressive stress in the
512 slabs and some bending was detected during the tests. In the configuration used for this study,
513 it was not possible to perform the direct measurement with the double-cell, but the results for
514 each technique can be compared and analysed in regard to the literature.

515 Table 3 gives mean values obtained with the three non-destructive techniques for all the
516 compressive stresses performed in the study. Not all the slabs were investigated at all the
517 stresses. Most of the mean values were evaluated on 2 or 4 slabs. The measurements were
518 performed for only one slab for columns marked with an asterisk in Table 3.

519 *Table 3: Mean value from the different techniques on slabs under compressive stress (measurements performed*
520 *on 5 slabs – B1-1, B1-2, B1-3, B2-6 and B3-8, not all the 6 stresses were performed for all the slabs; columns*
521 *marked with asterisks indicate that only one slab was measured for this stress state)*

Stress	**(MPa)**	**0**	**0.5**	**2***	**4**	**8**	**12***
Surf. Perm.	$x10^{-17}$ m^2	1.4	1.2	1.2	2.2	1.2	-
Permittivity	-	9.0	9.5	-	8.8	9.3	9.2
Deduc. Sr	%	44.8	51.4	-	42.7	46.9	46.8
Resistivity	$\Omega.m$	219.6	227.0	234.0	273.1	246.3	289.3
Deduc. Sr	%	62.4	60.8	60.0	57.3	59.1	59.8

522

523 The value obtained by the three techniques for each slab was used to evaluate the apparent
524 permeability based on the calibration performed in Section 3 (Figure 12).

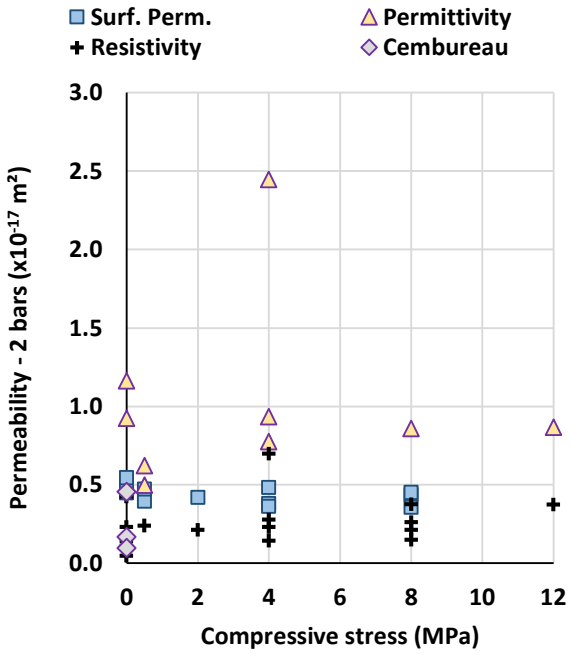

525

526 *Figure 12: Evaluation of apparent permeability at 2 bars given by the different techniques on slabs under*
527 *mechanical loading*

528 Surface permeability gave a correct evaluation of the apparent permeability compared to
529 reference measurements.

530 Permittivity measurements evaluated the saturation degree of the slabs at between 33.5% and
531 52.5% for specific values (the mean values were between 42.7% and 51.4% – Table 3) while
532 it was controlled at close to 60% by the pre-conditioning. The difference may have been due
533 to imperfect homogenization of the saturation in the slabs in spite of the specific conditioning.
534 Due to the difference of the speed of water movement in concrete between sorption and
535 desorption, homogenization is slower than drying [41]. If the same duration is used for drying
536 and homogenization, as is usually recommended for such measurements, the saturation
537 gradient is not totally removed at the end of the conditioning and the surface saturation is
538 lower than the core saturation. As permittivity apparatus investigated to about 15 mm in
539 depth, the underestimation could be partially explained by the remaining internal water

gradient. This underestimate led to an overestimate of the apparent permeability, particularly for one slab at 4 MPa.

Resistivity led to specific saturation degrees lying between 48.5 and 73% (between 57.3 and 60.8% for mean value) and, thus, the evaluation of apparent permeability through van Genuchten's law was in accordance with Cembureau measurements.

None of the three techniques was sufficiently precise to reliably demonstrate the decrease of air permeability with the increase of the compressive stress.

3.2.3 Impact of thermal loading

In this part, slabs at an initial saturation of 60% (and thus preconditioned at 50 °C) were subjected to 80 °C for 14 hours. At the end of the heating, the global saturation remained unchanged (verification by weighing of the slabs). The loading can thus be considered as a thermal load of 30 °C. However, internal water movements could have occurred during the heating.

Two slabs were used for this part. Results obtained for the three non-destructive techniques and for the direct measurement with the double-cell technique for one slab are given in Table 4.

Table 4: Measurements from the different techniques on slabs after thermal loading of 30 °C

	Slab	**B2-8**		**B3-8**	
Temperature	*°C*	**50**	**80**	**50**	**80**
Surf. Perm.	$x10^{-17}$ *m²*	1.10	2.18	1.46	2.89
Permittivity	-	10.1	11.4	9.2	11.7
Deduc. Sr	*%*	55.6	68.3	46.1	72.0
Resistivity	*Ω.m*	177.0	186.2	157.0	149.5
Deduc. Sr	*%*	67.0	65.7	70.2	71.6
Double-cell	$x10^{-17}$ *m²*		1.8		

The results were then used to evaluate the apparent permeability (Figure 13) just after the preconditioning at 50 °C and after the thermal heating at 80 °C. Permeability was also measured with the Cembureau technique on usual laboratory samples for the same thermal loading with the same conditioning used for the slabs. Complementary saturation degrees were also investigated to understand the underlying mechanisms better. The results were presented and analysed in [22]. Permeability of concrete exposed to 80 °C for 14 hours was almost twice that of concrete dried at 50 °C for an initial saturation degree of 60%. This can be explained by physicochemical reactions (decomposition of hydrates) or by the cracking induced by the differential dilation of aggregate and cement paste [47–50]. The results obtained on samples with the Cembureau technique have been added to Figure 13 for comparison with measurements performed on slabs.

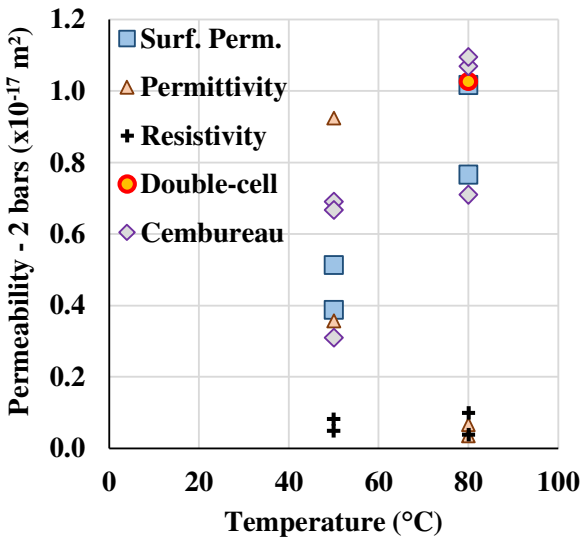

Figure 13: Evaluation of apparent permeability at 2 bars with the different techniques on slabs after a thermal loading of 30 °C

The three techniques of permeability measurements (surface permeability, Cembureau and double-cell) were consistent with the usual scatter found with such techniques.

574 Permittivity gave an evaluation consistent with the permeability technique at 50 °C but the
575 evaluation after the thermal loading at 80 °C was very low. For this case, the technique
576 evaluated the saturation degree as lying between 68% and 72% while it was between 46% and
577 55% at 50 °C (Table 4). In this domain, van Genuchten's law is very non-linear and a small
578 difference in permittivity measurement leads to a great difference in permeability evaluation.
579 As the water content was not modified during the heating, a similar permittivity was expected.

580 The same conclusion can be drawn for resistivity measurement. Resistivity led to saturation
581 degrees lying between 65% and 72% for the two slabs in the two states, which resulted in
582 very low apparent permeability. It was not consistent with permeability measurements
583 performed on the slab but, with apparent permeability of about 0.1 x 10^{-17} m², it remains
584 consistent with the apparent permeability measured on specimens with high saturation degree
585 (Figure 5).

586 In this part, the two electrical techniques seem to lead to an overestimation of the saturation
587 degree. The difference between the saturation degree obtained by these techniques and the
588 global saturation degree obtained by mass measurement can be explained by imperfect
589 homogenization of the saturation in the slabs in spite of the specific conditioning as explained
590 in the previous part. These slight overestimations of the saturation degree had an important
591 impact (one order of magnitude) on the predicted permeability obtained here due to the
592 accumulation of uncertainties. There was not a decimal order on the saturation. But as the
593 evolution of the permeability was quite scattered (factor 2 around 60% of saturation) and very
594 nonlinear in this domain, the prediction of the permeability led to this order of magnitude.
595 Therefore, direct permeability measurements are the most reliable techniques to obtain the
596 most accurate evaluation of the permeability.

Permittivity and resistivity were not sensitive to the damage induced by the thermal loading for the high saturation degree of 60%. This confirms the observations made on cores (Figure 7-b and Figure 9-b).

3.2.4 Impact of thermo-hydric loading

Slabs at 60% of initial saturation were subjected to 150 °C and 200 °C for 14 hours. At the end of the heating, the slabs were almost dry (in spite of the aluminium wrapping). The slabs exposed to 150 °C lost slightly less water mass than the slabs exposed to 200 °C. The loading can thus be considered as thermo-hydric, due to variations of temperature of 100 °C and 150 °C. Such temperatures are usually used to represent accidental conditions in enclosure vessels [51].

Resistivity cannot be measured for dry concrete and thus Table 5 presents the experimental results for the two other local non-destructive techniques and for the direct measurement by double-cell in a vacuum.

Table 5: Measurements from the different techniques on slabs after thermo-hydric loading

	Slab	**B2-10**	**B3-10**	**B2-9**	**B3-9**
Temperature	*°C*	**150**	**150**	**200**	**200**
Surf. Perm.	$x10^{-17}$ *m²*	30.6	45.1	47.3	56.5
Permittivity	-	5.0	4.8	4.7	4.8
Deduc. Sr		5.1	2.9	1.8	2.6
Double-cell	$x10^{-17}$ *m²*	11.8		46.0	

Apparent permeability was then evaluated as described previously and represented in Figure 14. At 150 °C, the evaluation given by surface permeability and permittivity was in good accordance and consistent with the Cembureau measurement. When compared to the direct measurement performed by double-cell, the three techniques overestimated the permeability.

At 200 °C, the evaluation performed with the three permeability techniques (surface measurement, double-cell and Cembureau technique on samples) were quite scattered but centred on the value determined by double-cell. The permittivity did not show significant evolution between the two loadings (150 °C and 200 °C) and underestimated the permeability. At the end of the thermo-hydric loading, the water content in the concrete was very low and permittivity measurement was not sensitive to the evolution of transfer paths.

For such conditions (thermo-hydric loading with exposure at 150 °C and 200 °C), concrete slabs should have been significantly damaged [52,53]. Cracking is a random phenomenon and can increase the usual heterogeneity of concrete. This can explain an increase of scatter on the measurements after loading leading to cracking. The dimensions of the surface permeameter (diameter of 40 mm for the measurement cell), designed first to evaluate permeability of the cover concrete, led to a limited representative volume during measurement. This can increase the impact of material heterogeneity on the permeability evaluation.

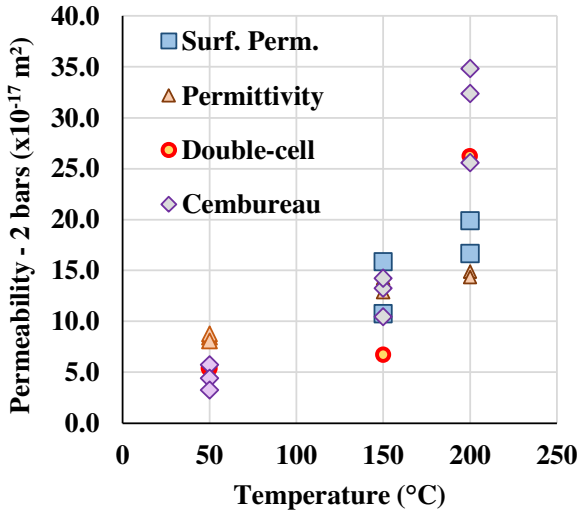

Figure 14: Evaluation of apparent permeability at 2 bars with the different techniques on slabs after thermal hydric loading

3.3 Application to real structures: concrete permeability of Vercors mock-up

3.3.1 In situ measurements

In this part, the three non-destructive techniques are applied to evaluate the permeability of the concrete of the Vercors structure. This structure is the mock-up of a reactor containment at 1/3 scale. It was built by EDF to help with the management of the long-term operation of its fleet of Nuclear Power Plants [19].

The aim was to compare the evaluation of the concrete permeability by three techniques that can be used in the field. Eighty measurements were performed with the surface permeameter and with the permittivity technique in the same locations of the structure on two horizontal lines around the mock-up and three vertical lines representative of the mock-up (Figure 15). These measurements were taken after the usual exposure of the surfaces of the mock-up to water performed during each enclosure test in order to detect singular air flow. This is an important point as it can impact the experimental results. Before the water sprinkling, skin concrete was sufficiently dry to prevent resistivity from being measured for most of the measurement locations. After sprinkling, some resistivity measurements were made in 27 locations, but, as shown in the following part, most of the measurements were higher than 300 Ω.m and, thus, in a domain where the results are usually quite scattered (Figure 9) and not very precise.

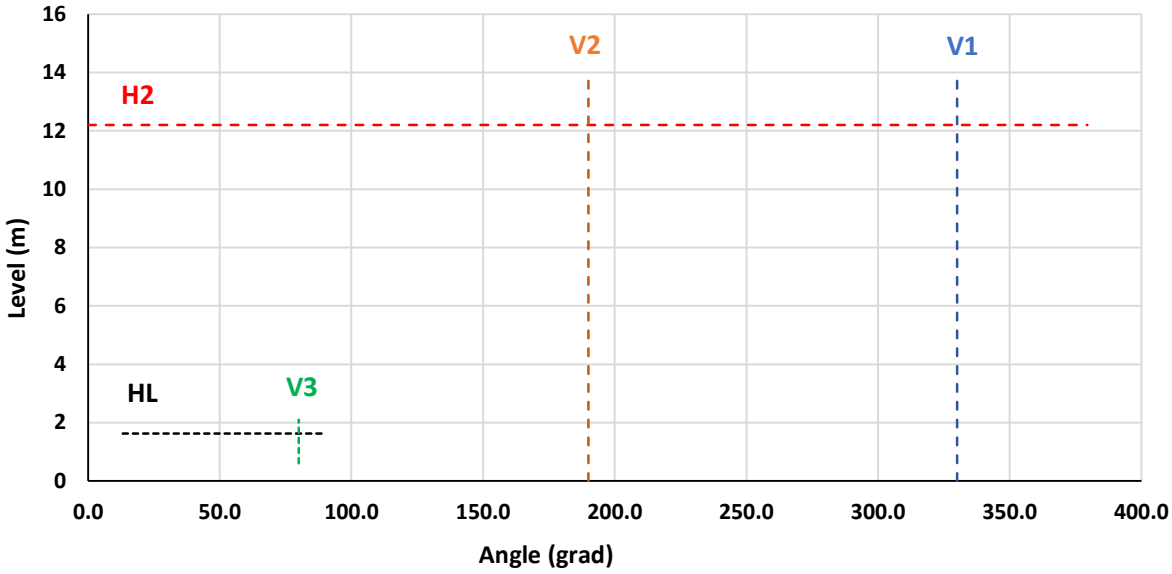

Figure 15: Locations of the measurements points along two horizontal and three vertical lines of the mock-up

As the mock-up has been realized for engineering and research work, particular attention was given to obtain the same reproducible material during the construction. All the measurements performed in this paper were located on the same face of the containment and protected from direct rain by the external wall and by the dome. Thus, the reasons for the discrepancy due to location of measurement were limited in this application.

Figure 16, Figure 17 and Figure 18 represent the distributions of surface permeability, permittivity and resistivity, respectively, measured on the mock-up. It has been chosen to present first the measurement results as histograms. This makes it possible to have a global view of the results and to estimate that the discrepancy stays quite small even if different castings were realized. These data can also be helpful for researchers interested in probabilistic approaches. In the following part, the permeability deduced from these measurements is presented by distribution along the five measurements lines to evaluate the discrepancy according to measurement location.

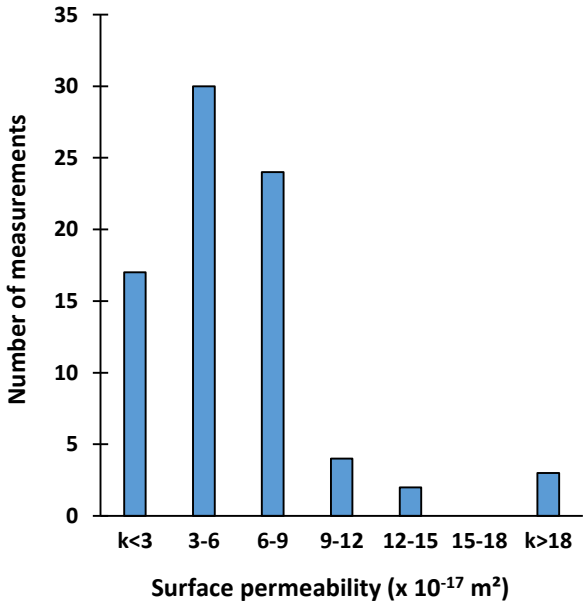

666

667 *Figure 16: Measurement of surface permeability on mock-up (80 values – mean: 5.9 x 10^{-17} m², min: 0.41 x 10^{-17} m², max 27.6 x 10^{-17} m²)*

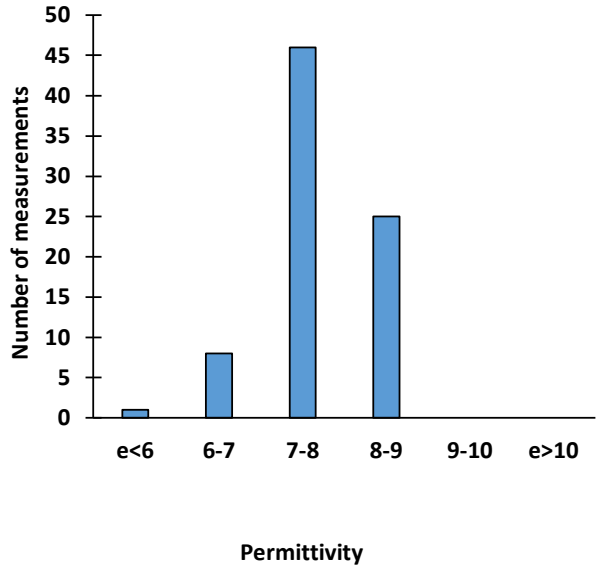

669

670 *Figure 17: Measurement of permittivity on mock-up (80 values – mean: 7.70, min: 5.60, max: 8.73)*

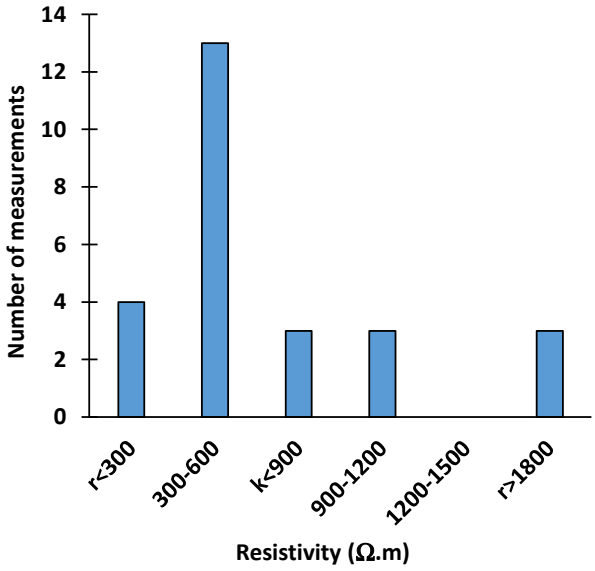

671

672 *Figure 18: Measurement of resistivity on mock-up (27 values – mean: 970 Ω.m, min: 233 Ω.m, max: 5471 Ω.m)*

673 *3.3.2 Evaluation of the saturation degree*

674 Permittivity and resistivity were used first to evaluate the saturation degree (Table 6). From
675 the calibration performed on the samples, the saturation degree evaluated by permittivity on
676 the mock-up lay between 12% and 42%, with a mean value of about 31.5% for the 80
677 measurement points, while resistivity gave a mean saturation degree of about 42.6% on 27
678 measurement points. The mean saturation degree evaluated by the permittivity on the same 27
679 points was about 29.8%. Thus, the difference of results is not a problem of the locations of the
680 measurement points but really a difference between the responses of the two techniques.

681 *Table 6: Saturation degree deduced from permittivity and resistivity*

	By permittivity	By resistivity
Min	12.1	17.3
Mean	**31.6**	**42.6**
Max	41.9	60.1
N° of values	80	27

682

683 The surface permeability can also give interesting information about the saturation degree.
684 With this aim in mind, the mean increase of pressure, $\dot{P}_c$, was evaluated for the 80
685 measurements performed on the mock-up and compared to the measurements performed on

laboratory samples. The mean $\dot{P}_c$ was equal to 2.2, which corresponds to a concrete saturated at about 40% of saturation for the laboratory samples.

Resistivity measurement was very sensitive to the saturation [12,13,17,18]. Below 40% of saturation, the continuity of the solution in concrete porosity was not sufficient to give a reliable response. For dry concrete with small saturation (lower than 40%), permittivity presents more precise results, because the measurement does not depend on the continuity of the solution but only on the water content. The tests were performed during an enclosure test and, thus, just after the water sprinkling of the concrete surface, water saturated a small thickness of concrete (probably some millimetres – Figure 19). It was just enough to have a superficial continuity of the concrete solution and thus to measure the resistivity. In this situation, the measurement probably represents the saturation of only the first few millimetres of the concrete skin. Permittivity is not influenced by the continuity of measurement. With the apparatus used in this work, permittivity was measured over about 15 mm of depth (Figure 19). As the water due to the sprinkling did not have time to penetrate the concrete, the saturation degree given by the permittivity was smaller but representative of a larger thickness of concrete. Finally, the measurement of surface permeability investigated thicknesses lying between 50 and 100 mm. For such thicknesses, the technique integrates the saturation degree of the skin and also the saturation degree of deeper concrete, for which the saturation degree is higher (Figure 19).

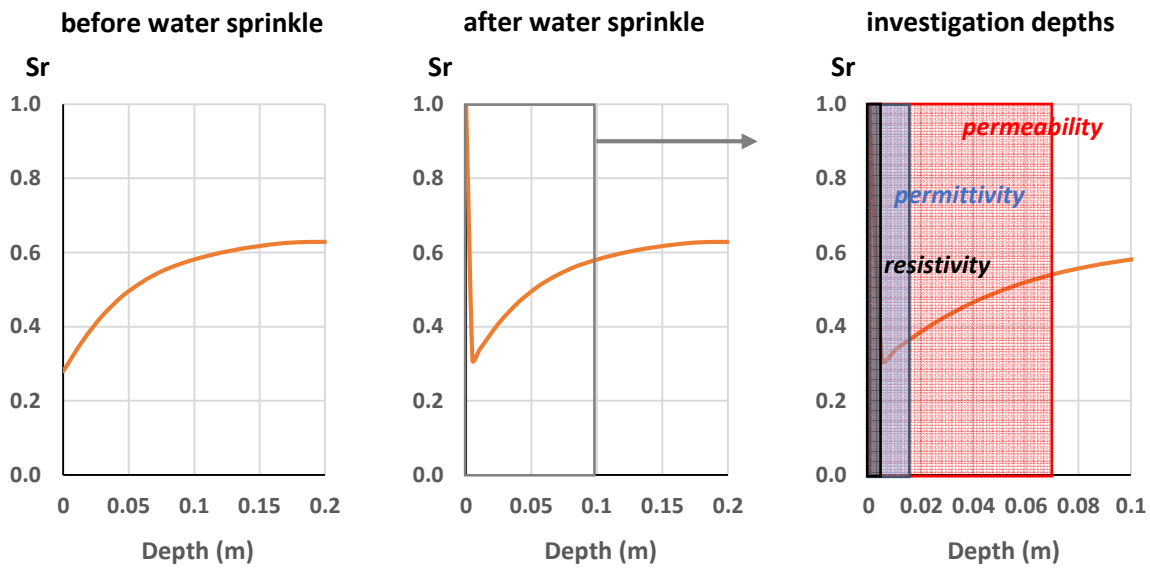

(a) (b) (c)

706 *Figure 19: Gradient of water content of a half depth of the mock-up wall (total depth: 0.4 m) before water*
707 *sprinkling* [20] *(a), approximate gradient after water sprinkling (b), and approximate depths of investigation for*
708 *the three techniques (c)*

709

710 *3.3.3 Evaluation of apparent permeability*

711 Then, the concrete apparent permeability for an absolute pressure of 2 bars was evaluated
712 from the measurements obtained with the three techniques. The permeability deduced from
713 the three techniques is presented along the two horizontal lines (Figure 20) and the three
714 vertical lines (Figure 21). Minimum, mean and maximum values of this evaluation are given
715 in Table 7.

716

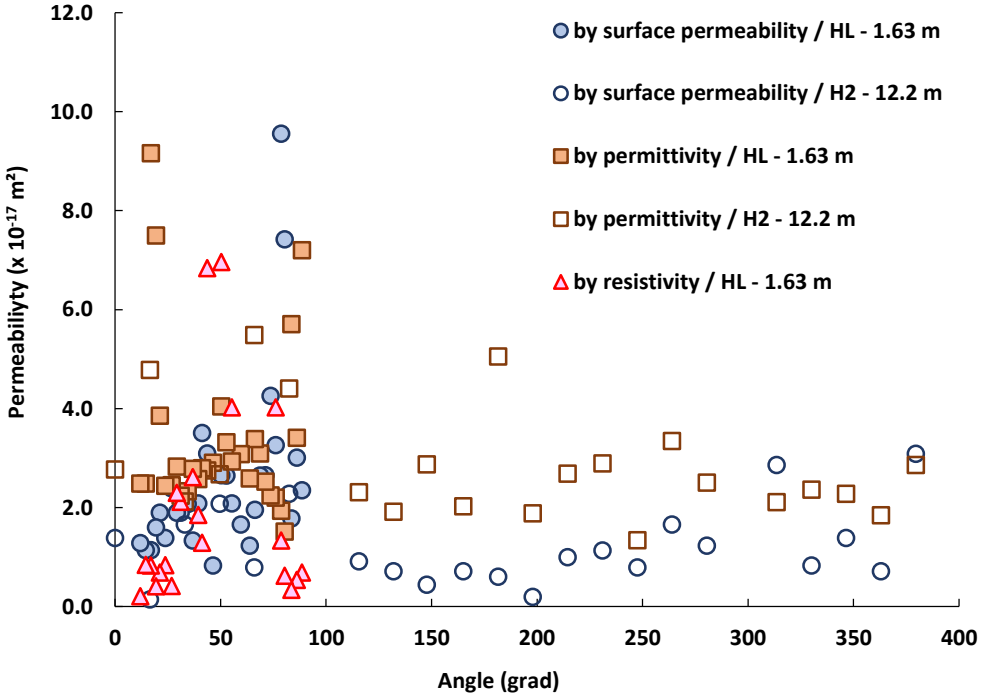

717

718 *Figure 20: Distribution of the permeability deduced from surface permeameter, permittivity and resistivity*
719 *measurements along the two horizontal lines*

720

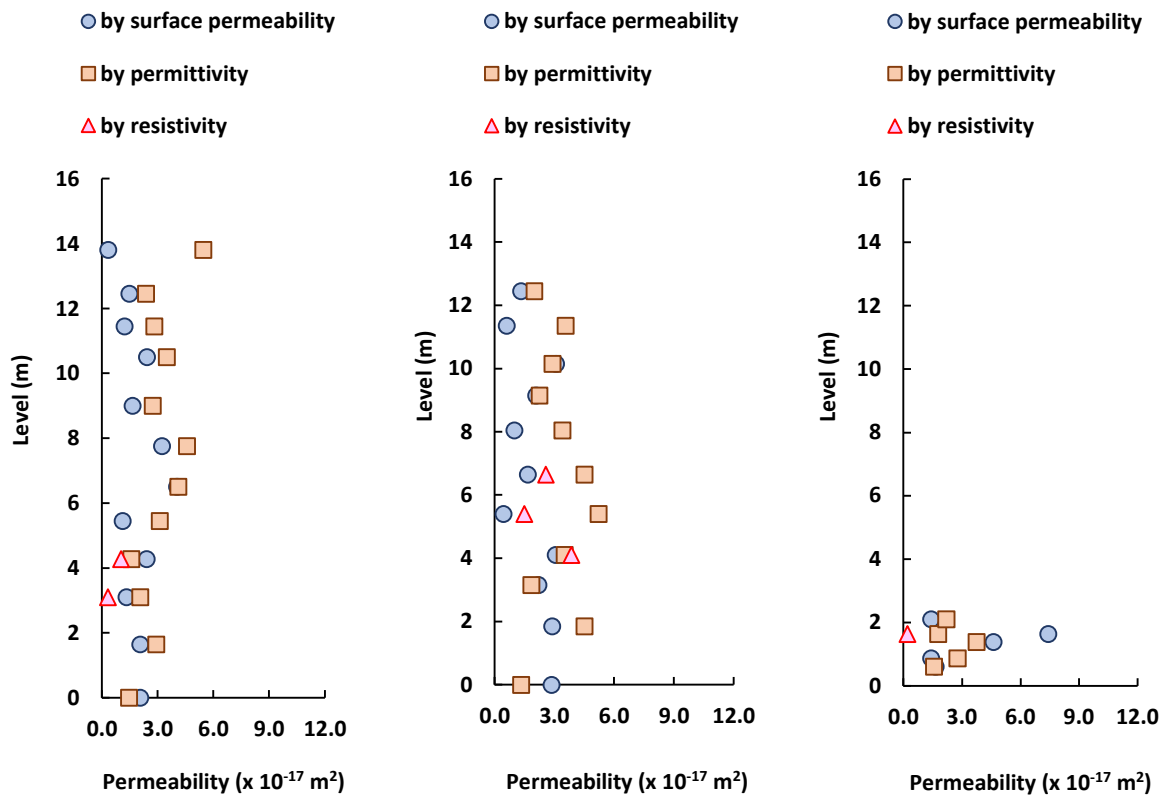

(a) (b) (c)

721 *Figure 21: Distribution of the permeability deduced from surface permeameter, permittivity and resistivity*
722 *measurements along the three vertical lines (a: V1, b: V2 and c: V3)*

723

724 *Table 7: Apparent permeability of the mock-up concrete evaluated by a surface permeameter, permittivity and*
725 *resistivity (x 10^{-17} m²)*

	By surf. perm.	By permittivity	By resistivity
min	0.14	1.33	0.21
mean	**2.06**	**3.1**	**1.7**
max	9.55	9.16	6.96
N° of values	80	80	27

726

727 Figure 20, Figure 21 and Table 7 highlight the difference in the evaluation of the permeability
728 by the three techniques.

729 With all the measurements, the surface permeability led to a mean apparent permeability of
730 about 2.06 x 10^{-17} m². Three points presented very large permeability (higher than 6. x 10^{-17}
731 m²). The two highest values were located on the horizontal line close to the angle 80 grad and

732 thus close to a rib for prestressing anchorages. They indicate a zone with poor transfer
733 resistance. This is consistent with permittivity measurement which shows a small saturation
734 degree in this part of the mock-up. The evaluation performed from the permittivity
735 measurements led to greater values of permeability in most of the measurement points. The
736 results were consistent with the results in the laboratory: with saturation of about 30%, the
737 concrete permeability can be expected to be between 3 and 4 x 10^{-17} m² (Figure 5). The two
738 highest values of permittivity were located on the horizontal line close to the angle 20 grad,
739 but the other measurements do not show extreme values in this zone. The distribution
740 obtained for the resistivity was mainly in the range of the smallest apparent permeability
741 obtained with the surface permeameter. The mean value for 27 points was about 1.73 x 10^{-17}
742 m². The horizontal distribution of the permeability deduced from resistivity shows abrupt
743 variations with angle. It can be due to the limit observed in laboratory: for dry concrete,
744 resistivity is highly non-linear with the saturation degree and the dispersion of the
745 measurement increases.
746 Therefore, the mean values of apparent permeability given by the three techniques were quite
747 close: the permittivity predicted an apparent permeability 35% greater than the surface
748 permeameter and the resistivity gave a permeability 25% smaller than the permeameter
749 technique. As discussed in the previous section, the differences may have come from the
750 depth investigated by each technique (some millimetres of skin due to water sprinkling for
751 resistivity, about 15 mm for the permittivity and more than 50 mm for the permeameter -
752 Figure 18).

753 # 4 Discussion

754 The work of the first step on laboratory specimens, confirmed the interest of three non-
755 destructive techniques (surface permeameter, permittivity, resistivity) for the evaluation of the
756 air permeability and saturation degree of concrete. Permittivity and resistivity depend on the

757 water content of the concrete and can thus be useful to evaluate the saturation degree [54,55].
758 Such an evaluation combined with van Genuchten's law, calibrated on laboratory specimens
759 by the Cembureau technique, allows the indirect evaluation of air permeability of concrete in
760 the field. In the second step, on laboratory slabs, the three techniques were used in the
761 laboratory for slabs of large dimensions and were compared with direct measurements of
762 permeability developed especially for this programme. In spite of some discrepancies, the
763 comparative analysis highlighted the consistent results for the different techniques. The third
764 step aimed to use the three techniques on a mock-up of a reactor containment at 1/3 scale. As
765 the measurements were made after exposure of the surfaces of the mock-up to water to detect
766 singular air flow during the enclosure test, the conditions of moisture according to concrete
767 depth were not in equilibrium with external conditions and the concrete skin presented a
768 strong humidity gradient (Figure 18). This is an important difference with investigations on
769 slabs, which were set up to have conditions that were as homogeneous as possible. It is
770 important to note that each technique investigates different depths of concrete. The
771 combination between moisture gradient and difference of investigation depth can partly
772 explain the small differences between the mean apparent permeability obtained with the three
773 techniques.
774 The problem of investigated depth is important to perform relevant expertise. In a massive
775 structure, water content is not homogeneous. Important moisture gradients exist between the
776 core and the skin. Close to the external limit, the saturation degree decreases abruptly.
777 Currently, no experimental technique is able to evaluate a gradient of moisture in the depth of
778 a concrete wall. Increasing the investigated depth would lead to average measurement results.
779 The result would not be more precise and would stay difficult to interpret without modelling.

In this mock-up, reinforcement bars were located at about 20 mm of the external skin. Steel bars can disturb the results of electrical methods [56,57]. Thus, the equipment was chosen to decrease the risk of disturbance by steel bars and to investigate less than 20 mm [58].

For such strategic structures, measurements cannot be the only way for expertise. They should be combined with numerical modelling through global methodology to precisely evaluate the moisture gradient through the wall [59,60]. In such approaches, the precise knowledge of the moisture conditions, even at 10 mm depth, is very important to avoid assumptions which are difficult to verify [60]. A few years ago, this type of evaluation required destructive sawing techniques [59]. They led to a certain degradation of the structure which is not acceptable for nuclear containment buildings. Resistivity for concrete exposed to high moisture conditions and permittivity in most cases can lead to evaluate the water content close to concrete skin without degradation of the concrete. It is an important improvement to control the boundary conditions imposed in modelling.

Finally, air flow through structural concrete is the combination of diffuse flow through the concrete and singular flow through preferential paths due to casting joints (caused by the manufacturing of the mock-up in several stages) or cracks. The first objective of the surface permeameter is to evaluate the diffuse flow, but it can also give interesting data to evaluate small singular flows. These techniques allowed the apparent permeability of the concrete skin to be evaluated. In the core of the concrete structure, the saturation degree is higher and the flow through the enclosure vessel has to be evaluated with a realistic moisture gradient in the wall.

5 Conclusion

The aims of this experimental work were to compare the response of three non-destructive techniques to, directly or indirectly, evaluate the air permeability of concrete in containment structures in laboratory and in field during the service life and after accidental conditions.

In laboratory conditions:

- For most of the situations, the three techniques of permeability measurement based on an air flow evaluation (global measurement with double cell, evaluation on representative specimens by Cembureau, and surface permeameter) were in good agreement with respect to concrete heterogeneity (most differences are less than 50%). The double cell technique is of great interest to evaluate the permeability in steady state for elements of large size. It has thus been shown that the apparent pressure for an absolute pressure of 2 bars can be evaluated from surface permeability measured in vacuum.
- Both electrical measurement techniques (permittivity and resistivity) give consistent values of concrete saturation degrees for values above 60% RH but are strongly dependent on this saturation, especially near this value. Under 60%, resistivity shows high dispersion and particular attention should be paid to the analysis of this measurement for concrete under such conditions. Permittivity can be used for all ranges of saturation, from totally saturated to dry concrete. Under 20% of saturation, this technique seemed to be more sensitive to small changes in the concrete or in the environmental conditions during tests. Meanwhile such degree of saturation is rarely encountered for real reinforced concrete structures in normal conditions of service.
- The prediction of permeability by the two electrical techniques can lead to great scattering due to the accumulation of uncertainties when their measurements were combined with van Genuchten's law evaluated with the Cembureau technique on

827 specimens. The scattering can be explained by the sensitivity of the techniques to
828 saturation degree and by the high nonlinearity of concrete permeability with the
829 saturation degree.
830 - Accidental conditions led to very low saturation degrees in concrete slabs. Resistivity
831 could not be used and permittivity was no more so precise. Surface permeameter
832 underestimated the permeability compared to double cell technique. It can be due to an
833 increase of heterogeneity due to cracking induced by the thermal loading.
834 For the use on a mock-up of a reactor containment at 1/3 scale:
835 - Surface permeameter gave a precise mapping of the distribution of permeability along
836 two horizontal and three vertical lines. The transfer property was quite homogeneous
837 in the structure except close to a singularity (presence of prestressing anchorages).
838 - The concrete skin presented a strong humidity gradient (Figure 18). However, from
839 the saturation degree evaluated with permittivity and resistivity, it was possible to
840 evaluate the apparent permeability of concrete skin by means of a van Genuchten law
841 calibrated in the laboratory on representative samples of the structural concrete. This
842 method gave interesting results on the mock-up when compared to the surface
843 permeability measurements.
844 - The combination of these two non-destructive electrical techniques with a surface
845 permeameter helps to provide a better understanding of the saturation state of the
846 concrete in the field. However, for accurate measurements of concrete permeability in
847 field, the present work highlights the need to use a surface permeameter. Electrical
848 techniques lead to correct evaluation of the degree of saturation in field. But the
849 accumulation of uncertainties can lead to large scattering for the prediction of the
850 permeability by such techniques especially close to their domain of use.

- Even if the saturation degree can only be measured for small investigated depth with resistivity and permittivity, it is a crucial data to help modelling to have realistic boundary conditions for calculations of moisture transfer in concrete structures.

6 Acknowledgements

The authors acknowledge the financial support provided by the project "Non-destructive evaluation of containment of nuclear power plants" (ENDE) financed by the Programme Investissement d'Avenir (PIA – Centre National de la Recherche Scientifique, délégation Provence et Corse, France). The opinions presented in this paper reflect only those of the authors and do not necessarily represent the opinions of the funding agencies.

7 References

[1] IAEA, Ageing Management of Concrete Structures in Nuclear Power Plants, 2016. https://www.iaea.org/publications/10659/ageing-management-of-concrete-structures-in-nuclear-power-plants.

[2] W. Kubissa, M.A. Glinicki, M. Dąbrowski, Permeability testing of radiation shielding concrete manufactured at industrial scale, Mater. Struct. 51 (2018) 83.

[3] J.J. Kollek, The determination of the permeability of concrete to oxygen by the Cembureau method-a recommendation, Mater. Struct. 22 (1989) 225–230. https://doi.org/10.1007/BF02472192.

[4] R.J. Torrent, A two-chamber vacuum cell for measuring the coefficient of permeability to air of the concrete cover on site, Mater. Struct. 25 (1992) 358–365.

[5] P. Basheer, F. Montgomery, A. Long, "CLAM" tests for measuring in situ permeation properties of concrete, Nondestruct. Test. Eval. 12 (1995) 53–73.

[6] Z. Lafhaj, G. Richard, M. Kaczmarek, F. Skoczylas, Experimental determination of intrinsic permeability of limestone and concrete: Comparison between in situ and laboratory results, Build. Environ. 42 (2007) 3042–3050. https://doi.org/10.1016/j.buildenv.2006.07.039.

[7] J. Liu, F. Agostini, F. Skoczylas, From relative gas permeability to in situ saturation measurements, Constr. Build. Mater. 40 (2013) 882–890. https://doi.org/10.1016/j.conbuildmat.2012.11.092.

[8] K. Yang, P.A.M. Basheer, Y. Bai, B.J. Magee, A.E. Long, Development of a new in situ test method to measure the air permeability of high performance concretes, NDT E Int. 64 (2014) 30–40. https://doi.org/10.1016/j.ndteint.2014.02.005.

[9] R. Torrent, Measures the Air-Permeability of the Cover Concrete and other Porous, (2009).

886 [10] A. Abbas, M. Carcasses, J.-P. Ollivier, Gas permeability of concrete in relation to its
887 degree of saturation, Mater. Struct. 32 (1999) 3–8.

888 [11] G. Villain, V. Baroghel-Bouny, C. Kounkou, C. Hua, Mesure de la perméabilité aux
889 gaz en fonction du taux de saturation des bétons, Rev. Française Génie Civ. 5 (2001)
890 251–268. https://doi.org/10.1080/12795119.2001.9692306.

891 [12] G.E. Monfore, The electrical resistivity of concrete, J. PCA. (1968) 35–48.

892 [13] M. Saleem, M. Shameem, S. Hussain, M. Maslehuddin, Effect of moisture, chloride
893 and sulphate contamination on the electrical resistivity of Portland cement concrete,
894 Constr. Build. Mater. 10 (1996) 209–214.

895 [14] D. Smyl, Electrical tomography for characterizing transport properties in cement-based
896 materials: A review, Constr. Build. Mater. 244 (2020) 118299.

897 [15] X. Dérobert, J. Iaquinta, G. Klysz, J.P. Balayssac, Use of capacitive and GPR
898 techniques for the non-destructive evaluation of cover concrete, NDT E Int. 41 (2008)
899 44–52. https://doi.org/10.1016/j.ndteint.2007.06.004.

900 [16] G. Villain, A. Ihamouten, X. Dérobert, Determination of concrete water content by
901 coupling electromagnetic methods: Coaxial/cylindrical transition line with capacitive
902 probes, NDT E Int. 88 (2017) 59–70. https://doi.org/10.1016/j.ndteint.2017.02.004.

903 [17] S. Bonnet, J.P. Balayssac, Combination of the Wenner resistivimeter and Torrent
904 permeameter methods for assessing carbonation depth and saturation level of concrete,
905 Constr. Build. Mater. 188 (2018) 1149–1165.
906 https://doi.org/10.1016/j.conbuildmat.2018.07.151.

907 [18] Y.L. Yang, T. Zhang, S.Y. Liu, Influence factor analysis and calculation model for
908 thermal/electrical resistivity of geomaterials, Measurement. 152 (2020) 107373.
909 https://doi.org/10.1016/j.measurement.2019.107373.

910 [19] E. Oukhemanou, S. Desforges, E. Buchoud, S. Michel-Ponnelle, A. Courtois,
911 VeRCoRs Mock-Up: Comprehensive Monitoring System for Reduced Scale
912 Containment Model, in: Technol. Innov. Nucl. Civ. Eng. TINCE, Paris (France), 2016.

913 [20] L. Charpin, J. Niepceron, M. Galan, S. Desforges, VERCORS : vérification réaliste du
914 confinement des réacteurs. Jumeau numérique, instrumentation, in: Séminaire, Instrum.
915 Pour Le Diagnostic Des Constr. En Béton, ACI Paris, Fr., 2020.

916 [21] Z. Wu, H.S. Wong, N.R. Buenfeld, Influence of drying-induced microcracking and
917 related size effects on mass transport properties of concrete, Cem. Concr. Res. 68
918 (2015) 35–48. https://doi.org/10.1016/j.cemconres.2014.10.018.

919 [22] H. Sogbossi, J. Verdier, S. Multon, Permeability and damage of partially saturated
920 concrete exposed to elevated temperature, Cem. Concr. Compos. 109 (2020) 103563.
921 https://doi.org/10.1016/j.cemconcomp.2020.103563.

922 [23] H. Sogbossi, Etude de l'évolution de la perméabilité du béton en fonction de son
923 endommagement : transposition des résultats de laboratoire à la prédiction des débits de
924 fuite sur site, PhD thesis, Université de Toulouse, 2017.

925 [24] H. Sogbossi, J. Verdier, S. Multon, New approach for the measurement of gas
926 permeability and porosity accessible to gas in vacuum and under pressure, Cem. Concr.
927 Compos. 103 (2019) 59–70. https://doi.org/10.1016/j.cemconcomp.2019.04.032.

928 [25] D. Zhang, K. Li, Concrete gas permeability from different methods: Correlation
929 analysis, Cem. Concr. Compos. 104 (2019) 103379.
930 https://doi.org/10.1016/j.cemconcomp.2019.103379.

931 [26] Y. Qin, J. Liang, H. Yang, Z. Deng, Gas permeability of pervious concrete and its
932 implications on the application of pervious pavements, Measurement. 78 (2016) 104–
933 110. https://doi.org/10.1016/j.measurement.2015.09.055.

934 [27] J.-F. Lataste, G. Villain, J.-P. Balayssac, 4-Electrical Methods, in: V. Garnier, J.-P.
935 Balayssac (Eds.), Non-Destructive Test. Eval. Civ. Eng. Struct., Elsevier, London,
936 2018: pp. 138–172. https://doi.org/https://doi.org/10.1016/B978-1-78548-229-8.50004-
937 2.

938 [28] M. Fares, G. Villain, S. Bonnet, S. Palma Lopes, B. Thauvin, M. Thiery, Determining
939 chloride content profiles in concrete using an electrical resistivity tomography device,
940 Cem. Concr. Compos. 94 (2018) 315–326.
941 https://doi.org/10.1016/j.cemconcomp.2018.08.001.

942 [29] G. Villain, V. Garnier, M. Sbartaï, X. Derobert, J.-P. Balayssac, Development of a
943 calibration methodology to improve the on-site non-destructive evaluation of concrete
944 durability indicators, Mater. Struct. 51 (2018) 40. https://doi.org/10.1617/s11527-018-
945 1165-4.

946 [30] V. Waller, Relations entre composition des betons, exothermie en cours de prise et
947 resistance en compression, PhD Thesis, École Nationale des Ponts et Chaussées, 1999.

948 [31] L.J. Parrott, Moisture conditioning and transport properties of concrete test specimens,
949 Mater. Struct. 27 (1994) 460–468.

950 [32] C. Antón, M.A. Climent, G. de Vera, I. Sánchez, C. Andrade, An improved procedure
951 for obtaining and maintaining well characterized partial water saturation states on
952 concrete samples to be used for mass transport tests, Mater. Struct. 46 (2012) 1389–
953 1400.

954 [33] RILEM TC 116-PCD, Permeability of concrete as a criterion of its durability, final
955 report, Mater. Struct. 32 (1999) 163–173.

956 [34] M. Carcassès, A. Abbas, J.-P. Ollivier, J. Verdier, An optimised preconditioning
957 procedure for gas permeability measurement, Mater. Struct. 35 (2001) 22–27.

958 [35] V. Garnier, C. Payan, L. Martin et al., Non-destructive evaluation of containment walls
959 in nuclear power plants, in: 43rd Annu. Rev. Prog. Quant. Nondestruct. Eval. Vol. 36,
960 AIP Conf. Proc., 2017: p. 1806(1):080018.

961 [36] M.T. van Genuchten, A Closed-form Equation for Predicting the Hydraulic
962 Conductivity of Unsaturated Soils, Soil Sci. Soc. Am. J. 44 (1980) 892.
963 https://doi.org/10.2136/sssaj1980.03615995004400050002x.

964 [37] J.P. Monlouis-Bonnaire, J. Verdier, B. Perrin, Prediction of the relative permeability to
965 gas flow of cement-based materials, Cem. Concr. Res. 34 (2004) 737–744.
966 https://doi.org/10.1016/S0008-8846(03)00071-1.

967 [38] M.P. Yssorche, J.P. Bigas, J.P. Ollivier, Mesure de la perméabilité à l'air des bétons au
968 moyen d'un perméamètre à charge variable, Mater. Struct. 28 (1995) 401–405.
969 https://doi.org/10.1007/BF02473075.

970 [39] V. Čalogović, Gas permeability measurement of porous materials (concrete) by time-
971 variable pressure difference method, Cem. Concr. Res. 25 (1995) 1054–1062.

972 [40] S. Dushman, J.M. Lafferty, S.C. Brown, Scientific foundations of vacuum technique,
973 Am. J. Phys. 30 (1962) 612–612.

974 [41] M. Abdou Ibro, Vers la prédiction des cinétiques de rééquilibrage entre 2 milieux
975 initialement en conditions de saturation différentes, PhD Thesis, Université de
976 Toulouse, France, 2020.

977 [42] D. Breysse, G. Villain, M.S. Zoubir, V. Garnier, 7 - Construction of Conversion
978 Models of Observables into Indicators, in: J.-P. Balayssac, V. Garnier (Eds.), Non-
979 Destructive Test. Eval. Civ. Eng. Struct., Elsevier, 2018: pp. 231–257.
980 https://doi.org//10.1016/B978-1-78548-229-8.50007-8.

981 [43] V. Guihard, F. Taillade, J.-P. Balayssac, B. Steck, J. Sanahuja, Permittivity
982 measurement of cementitious materials with an open-ended coaxial probe, Constr.
983 Build. Mater. 230 (2020) 116946. https://doi.org/10.1016/j.conbuildmat.2019.116946.

984 [44] M. Ibro, J. Verdier, S. Geoffroy, H. Cagnon, X. Bourbon, Prediction of moisture
985 transfer in cement-based materials : Use of a porous network model to access transfer
986 parameters, Cem. Concr. Res. 142 (2021) 106310.
987 https://doi.org/10.1016/j.cemconres.2020.106310.

988 [45] M. Choinska, A. Khelidj, G. Chatzigeorgiou, G. Pijaudier-cabot, Effects and
989 interactions of temperature and stress-level related damage on permeability of concrete,
990 Cem. Concr. Res. 37 (2007) 79–88. https://doi.org/10.1016/j.cemconres.2006.09.015.

991 [46] M. Hoseini, V. Bindiganavile, N. Banthia, The effect of mechanical stress on
992 permeability of concrete: A review, Cem. Concr. Compos. 31 (2009) 213–220.
993 https://doi.org/10.1016/j.cemconcomp.2009.02.003.

994 [47] Z.P. Bazant, Delayed thermal dilatations of cement paste and concrete due to mass
995 transport, Nucl. Eng. Des. 14 (1970) 308–318.

996 [48] F.E. Heuze, High-temperature mechanical, physical and Thermal properties of granitic
997 rocks - A review, Int. J. Rock Mech. Min. Sci. Geomech. Abstr. 20 (1983) 3–10.

998 [49] Z.P. Bazant, M.F. Kaplan, Concrete at High Temperatures: Materials Properties and
999 Mathematical Models, Longman, Burnt Mill, England, 1996.

1000 [50] S. Ghabezloo, Micromechanics analysis of thermal expansion and thermal
1001 pressurization of a hardened cement paste, Cem. Concr. Res. 41 (2011) 520–532.

1002 [51] S. Medjigbodo, A. Darquennes, C. Aubernon, A. Khelidj, A. Loukili, Effects of the air-
1003 steam mixture on the permeability of damaged concrete, Cem. Concr. Res. 54 (2013)
1004 98–105. https://doi.org/10.1016/j.cemconres.2013.08.013.

1005 [52] D. Gawin, C. Alonso, C. Andrade, C.E. Majorana, F. Pesavento, Effect of damage on
1006 permeability and hygro-thermal behaviour of HPCs at elevated temperatures: Part 1.
1007 Experimental results, Comput. Concr. 2 (2005) 189–202.
1008 https://doi.org/10.12989/cac.2005.2.3.189.

1009 [53] I. Yurtdas, N. Burlion, J.F. Shao, A. Li, Evolution of the mechanical behaviour of a
1010 high performance self-compacting concrete under drying, Cem. Concr. Compos. 33
1011 (2011) 380–388. https://doi.org/10.1016/j.cemconcomp.2010.12.002.

[54] R. Du Plooy, S. Palma Lopes, G. Villain, X. Dérobert, Development of a multi-ring resistivity cell and multi-electrode resistivity probe for investigation of cover concrete condition, NDT E Int. 54 (2013) 27–36. https://doi.org/10.1016/j.ndteint.2012.11.007.

[55] M. Fares, Y. Fargier, G. Villain, X. Derobert, S.P. Lopes, Determining the permittivity profile inside reinforced concrete using capacitive probes, NDT E Int. 79 (2016) 150–161. https://doi.org/10.1016/j.ndteint.2016.01.002.

[56] O. Sengul, O. Gjorv, Effect of embedded steel on electrical resistivity measurements on concrete structures, ACI Mater. J. 106 (2009) 11–18.

[57] M.-A. Alhajj, S.P. Palma Lopes, G. Villain, Accounting for steel rebar effect on resistivity profiles in view of reinforced concrete structure survey, Constr. Build. Mater. 223 (2019) 898–909. https://doi.org/10.1016/j.conbuildmat.2019.07.208.

[58] R. Polder, Test methods for on site measurement of resistivity of concrete- a RILEM TC-154 technical recommendation, Constr. Build. Mater. 15 (2001) 125–131.

[59] A. Sellier, E. Bourdarot, S. Multon, M. Cyr, E. Grimal, Combination of structural monitoring and laboratory tests for the assessment of AAR-swelling: application to a gate structure dam, ACI Mater. J. 106 (2009) 281–290.

[60] D. Vo, Stratégie de modélisation numérique du béton armé fissuré en contexte de dimensionnement ou de vériication des grands ouvrages de génie civil, PhD Thesis, Université de Toulouse, 2022.